ANTIOXIDANTS & REDOX SIGNALING
Volume 11, Number 5, 2009

DOI: 10.1089/ars.2008.2295

Original Research Communication

Dissecting the Oxidative Folding of Circular Cystine Knot Miniproteins

Sunithi Gunasekera, Norelle L. Daly, Richard J. Clark, and David J. Craik

Abstract

Cyclotides are plant proteins with exceptional stability owing to the presence of a cyclic backbone and three disulfide bonds arranged in a cystine knot motif. Accordingly, they have been proposed as templates to stabilize bioactive epitopes in drug-design applications. The two main subfamilies, referred to as the Möbius and bracelet cyclotides, require dramatically different *in vitro* folding conditions to achieve the native fold. To determine the underlying elements that influence cyclotide folding, we examined the *in vitro* folding of a suite of hybrid cyclotides based on combination of the Möbius cyclotide kalata B1 and the bracelet cyclotide cycloviolacin O1. The folding pathways of the two cyclotide subfamilies were found to be different and influenced by specific residues within intercysteine loops 2 and 6. Two changes in these loops, a substitution in loop 2 and an addition in loop 6, enabled the folding of a cycloviolacin O1 analogue under conditions in which folding does not occur *in vitro* for the native peptide. A key intermediate contains a native-like hairpin structure that appears to be a nucleation locus early in the folding process. Overall, these mechanistic findings on the folding of cyclotides are potentially valuable for the design of new drug leads. *Antioxid. Redox Signal.* 11, 971–980.

Introduction

The cyclotides (12) are the largest family of circular proteins currently known and contain a unique structural motif referred to as the cyclic cystine knot (CCK). This extremely stable motif is formed by the combination of a cyclic backbone and three conserved disulfide bonds arranged in a knotted topology. Several backbone loops project from the stable molecular core of cyclotides, as illustrated in Fig. 1. The primary function of cyclotides is thought to be as plant defense agents based on their potent insecticidal activity against the larvae of several *Helicoverpa* species (4, 25, 31, 32). However, cyclotides are functionally versatile and display a range of other bioactivities, including uterotonic (22–24), anti-HIV (27, 28), cytotoxic (35, 44), hemolytic (17, 30, 42, 46), antimicrobial (46), antifouling (21), nematicidal (10), and molluscicidal (38) activities. More than 100 cyclotides have been characterized (36, 47), with hypervariable sequences occupying the backbone loops. The combined features of exceptional stability, functional diversity, and an ability to tolerate a wide range of sequences make cyclotides potentially useful as molecular engineering templates onto which bioactive epitopes can be grafted and thereby stabilized (11, 14). Other peptides, such as knottins (8) and BPTI (39), have been used as scaffolds to graft nonnative activities, highlighting the potential of peptide scaffolds in drug design.

Two main cyclotide subfamilies have been defined: the Möbius and bracelet subfamilies, based on the geometry of an X-Pro peptide bond in the circular backbone (12). In Möbius cyclotides a *cis*-peptide bond in loop 5 results in a conceptual 180-degree twist in the backbone, as illustrated in Fig. 1. In contrast, bracelet cyclotides lack the corresponding proline residue and have a bracelet (all-*trans*) topology. Loops 1 and 4 of cyclotides form part of the cystine knot and are highly conserved across the two subfamilies. Despite some degree of sequence similarity within subfamilies, loops 2, 3, 5, and 6 vary in size and sequence across different cyclotides, as shown in Fig. 1. Based on the presence of a CCK topology (20), the two peptides *Momordica cochinchinensis* trypsin inhibitor I (MCoTI-I) and MCoTI-II, discovered in 2000 (29), constitute a

The University of Queensland, Institute for Molecular Bioscience and Australian Research Council Special Research Centre for Functional and Applied Genomics, Brisbane, Australia.

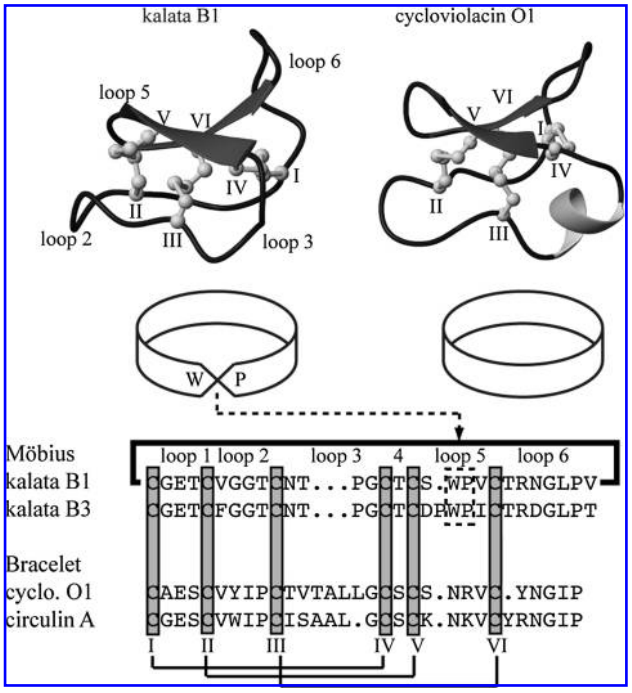

FIG. 1. Distinctive structural features of the Möbius and bracelet cyclotide subfamilies. A comparison of the three-dimensional structures of the prototypical Möbius cyclotide kalata B1 (*left*) and bracelet cyclotide cycloviolacin O1 (*right*) is shown; the three conserved disulfides forming the cystine knot are depicted in a *ball-and-stick model*, and the antiparallel β sheets are shown with *flat arrows*. The schematic diagram shows the Möbius and bracelet topologies; bracelet scaffold contains the conceptual twist between the Trp and Pro residue in loop 5. An alignment of sequences for representative members of each subfamily is shown at the bottom of the figure.

third cyclotide subfamily known as the trypsin-inhibitor cyclotides (13). These peptides are also referred to as "cyclic knottins," as they show high sequence similarity to linear trypsin inhibitors found within certain squash plants (7).

Möbius cyclotides can be efficiently synthesized by first assembling linear precursor sequences *via* solid-phase synthesis and then using a thioester-mediated strategy to generate the cyclic product (17, 46). Under alkaline folding conditions, cyclization and oxidation of the cysteines occur in a single step to give the natively folded conformation in high yields. Unlike conventional proteins that generally have hydrophobic residues in the protein core, native cyclotides have many of their hydrophobic residues exposed on the molecular surface. Inclusion of the hydrophobic agent isopropanol in the folding medium significantly increases the folding efficiency of the prototypical Möbius cyclotide kalata B1, presumably by stabilizing the patch of hydrophobic residues that is exposed to solvent on folding (17).

Despite the high yields obtained for folding of Möbius cyclotides, the folding of bracelet cyclotides has been problematic. In early studies of cyclotide synthesis, Tam *et al.* (45) reported that synthetic bracelet cyclotides require complex folding conditions and selective cysteine protection followed by directed oxidative folding to attain the native conformation. Recently, successful *in vitro* folding conditions for the bracelet cyclotide cycloviolacin O2 were reported that enabled folding yields up to ~50% (34). The optimal folding conditions were established after many attempts at folding under a wide range of conditions, including different buffer systems, temperatures, and metal ions, were unfruitful (1), indicating that folding of bracelet cyclotides is not as robust as that of Möbius cyclotides.

Grafting of bioactive sequences into cyclotide frameworks to derive biologically stable analogues has been proposed as a potential therapeutic application of cyclotides (11, 14). However, such applications have so far not been extended to members of the bracelet subfamily owing to the difficulties associated with their folding. More than 60% of the cyclotides discovered to date are bracelet cyclotides (43), and several NMR studies have confirmed that bracelet scaffolds possess naturally stable conformations (5, 32, 33, 37, 40), indicating that overall, the bracelet subfamily contains a large number of potential scaffolds available for protein-engineering applications. To optimize the range of cyclotide scaffolds used in drug-design applications, an understanding of the fundamental elements that dictate the *in vitro* folding of bracelet cyclotides is essential.

We examine the key structural features that influence the *in vitro* folding of the two main cyclotide subfamilies. To determine which backbone loops or key residues in cyclotides influence *in vitro* folding, we designed a suite of Möbius-bracelet hybrid cyclotides based on the prototypical Möbius and bracelet cyclotides kalata B1 and cycloviolacin O1, respectively. Our study indicates the structural elements that hinder the folding of bracelet cyclotides under conditions that are effective for Möbius counterparts and provides a new approach to folding of bracelet cyclotides by introducing simple modifications to the sequence.

Materials and Methods

Synthesis of Möbius-bracelet hybrids and native cycloviolacin O1

A series of bracelet-Möbius hybrids (hybrids 1–15) and native cycloviolacin O1 were assembled using Boc (*t*-butoxycarbonyl) chemistry (41) and purified by using methods previously described (9). In brief, peptides were assembled on a PAM (phenylacetamidomethyl) resin (Applied Biosystems, Foster City, CA) on a 0.3-mmol scale and were designed to contain a C-terminal thioester linker and an N-terminal cysteine (18). RP-HPLC was used to purify the peptides, and the fractions containing the correct mass detected by ESI-MS were freeze dried and used for the oxidative folding study.

Oxidative folding of hybrids. The hybrid peptides (0.1 mg/ml) were oxidized by using an array of nine small-scale *in vitro* folding oxidation buffers containing different proportions of 0.1 *M* ammonium bicarbonate (pH 8.5), isopropanol, and glutathione as shown in Table 1. The oxidative folding condition that gave a prominent peak in high yield for each peptide was repeated in large scale (total volume of 100 ml) for 24 h, and the folded peptide was purified on a semipreparative column by using a linear gradient of solvent A (0.1% aqueous trifluoroacetic acid) and B (0.05% trifluoroacetic acid in 90% acetonitrile/10% water). Fractions

Table 1. Standard Oxidation Conditions Used for Folding Cyclotides

Trial number	0.1 M ammonium bicarbonate (pH 8.5)	Isopropanol	Reduced glutathione	Oxidized glutathione
1	100%	–	–	–
2	100%	–	2 m*M*	–
3	100%	–	2 m*M*	0.4 m*M*
4	75%	25%	–	–
5	75%	25%	2 m*M*	–
6	75%	25%	2 m*M*	0.4 m*M*
7	50%	50%	–	–
8	50%	50%	2 m*M*	–
9	50%	50%	2 m*M*	0.4 m*M*

containing the correct mass were identified by ESI-MS and further analyzed with RP-HPLC for purity. Pure fractions (>95% purity) were freeze dried and examined with ^{1}H-NMR.

NMR experiments. Samples for ^{1}H-NMR measurements contained ~1 m*M* peptide in 90% water/10% ^2H_2O (vol/vol) at approximately pH 3. Spectra were recorded at 290 K on a Bruker ARX-600 spectrometer equipped with a shielded gradient unit. Additional spectra were acquired at 310 K for hybrid 8, hybrid 11, and hybrid 15. Two-dimensional NMR spectra were recorded as previously described (16). Chemical shifts were referenced to internal 2,2-dimethyl-2-silapentane-5-sulfonate.

Oxidative folding of cycloviolacin O1. Oxidative folding was carried out on the linear cycloviolacin O1 assembled with a thioester group and also on the base-treated linear chain from which the thioester group was removed. The thioester group was removed by incubating linear cycloviolacin O1 in 0.1 *M* potassium hydroxide (pH 11.5) for 10 min followed by purification on an RP-HPLC column.

Oxidative folding and reductive unfolding of hybrid 15. Purified hybrid 15 containing the thioester linker (0.5 mg/ml) was cyclized, and the cysteine residues were maintained in a reduced state by incubation in 0.1 *M* ammonium bicarbonate buffer (pH 8.5) containing sixfold excess Tris (carboxyethyl) phosphine hydrochloride for 45 min at 25°C. For oxidative folding, the purified reduced cyclic hybrid 15 was oxidized in oxidation condition 6. Aliquots were taken out at various time intervals, quenched with 0.4% TFA, and analyzed with analytic RP-HPLC. The major intermediate of hybrid 15 was captured by quenching with 0.4% TFA after 5 min of oxidative folding. The native hybrid 15 was obtained by quenching with 0.4% TFA after 24 h of oxidative folding. The intermediate and the native hybrid 15 were purified on RP-HPLC and characterized with ESI-MS and NMR. For reductive unfolding, purified native hybrid 15 (0.5 mg/ml) was reduced in ammonium bicarbonate buffer (pH 8.5) containing 25 m*M* dithiothreitol at 25°C. Aliquots were taken out at various time intervals, quenched with 0.4% TFA, and analyzed with analytic RP-HPLC.

Oxidative folding and reductive unfolding of kalata B8. Native kalata B8 was isolated from the aerial parts of *Oldenlandia affinis* plants by using a standard extraction procedure (16). The peptide (0.5 mg/ml) was reduced in 300 m*M* DTT containing ammonium bicarbonate buffer (pH 8.5) for 24 h at 25°C, purified on HPLC, and used for the oxidative folding study. Oxidative folding was carried out in standard oxidation condition 9, shown in Table 1. For reductive unfolding, a purified native species (0.1 mg/ml) was dissolved in 0.1 *M* ammonium bicarbonate (pH 8.0) containing 50 m*M* DTT at 25°C. Aliquots were removed at various time intervals, quenched with 0.4% TFA, and analyzed with analytic RP-HPLC.

Results

The main aim of the current study was to understand the reasons for poor folding of bracelet cyclotides under conditions in which Möbius cyclotides fold readily. To this end, we used a range of bracelet:Möbius hybrids to unravel the factors that influence the *in vitro* folding of cyclotides.

Cycloviolacin O1 is structurally well characterized and was chosen as the prototypical bracelet cyclotide for the investigation. We analyzed the oxidative folding of this cyclotide under a panel of standard oxidation conditions given in Table 1. Typically, native cyclotides elute late on RP-HPLC as a result of their surface-exposed patch of hydrophobic residues (17). The native form can readily be confirmed by ^{1}H-NMR analysis as cyclotides display well-dispersed NMR signals. Misfolded peptides usually give multiple overlapping peaks on RP-HPLC and do not have well-dispersed NMR signals.

In an initial series of experiments on the folding of cycloviolacin O1, only misfolded isomers were observed under the panel of conditions tested. To determine whether the folding could be improved if oxidation occurs before cyclization, we also examined the folding of the linear chain. However, the peptide still misfolded, indicating that even when disulfide bond formation occurred before the constraints imposed by cyclization, it was not possible to obtain correctly folded product (data not shown).

We then focussed on kalata B8, a natural hybrid between Möbius and bracelet subfamilies, to identify the "offender" loops responsible for the misfolding of bracelet cyclotides *in vitro*. In kalata B8, loops 2 and 3 closely resemble Möbius sequences, and loop 5 resembles bracelet cyclotides (16), as shown in Fig. 2. We found that kalata B8 readily folds into a native conformation *in vitro*, as shown in Fig. 2, which led to the proposal that loops 2 and 3 are likely to be the reason for the misfolding in bracelet cyclotides. A comparison of bracelet and Möbius sequences indicates that the amino acid sequences in loops 2 and 3 differ most significantly between the two subfamilies, supporting the proposal that bracelet loops 2 and 3 may have a major impact on folding. Thus, it was proposed that correct folding in cycloviolacin O1 may occur if loops 2 and 3 are substituted with the counterpart Möbius sequences.

We therefore designed a suite of hybrid peptides containing different loop combinations from both subfamilies, as shown in Fig. 3, with initial focus on loops 2 and 3. The Möbius cyclotide kalata B1 and bracelet cyclotide cycloviolacin O1 were used as the representative members for each cyclotide subfamily, as detailed structural data are available for both peptides (40). Hybrid 1 involves replacement of loop 2 of the cycloviolacin O1 sequence with the kalata B1 loop 2

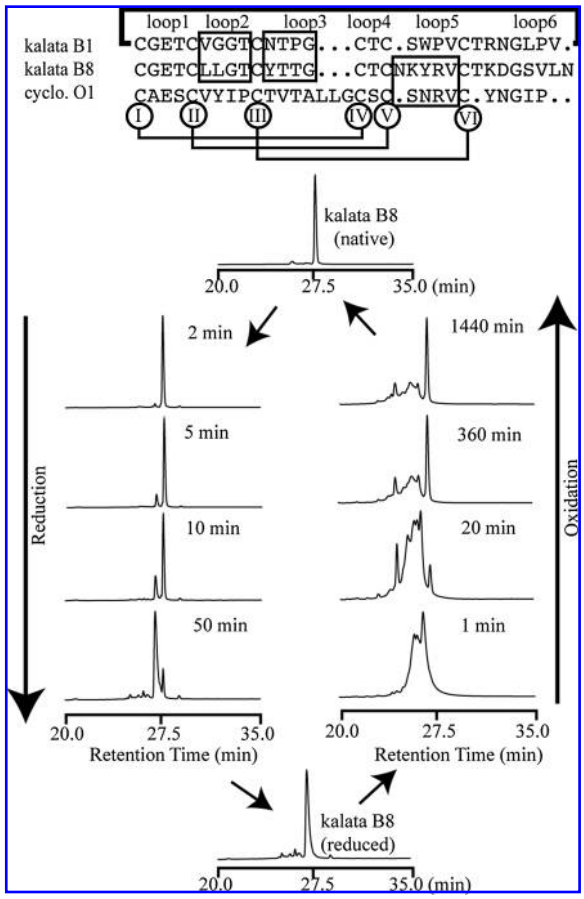

FIG. 2. Oxidative folding and reductive unfolding profiles of kalata B8. The sequence alignment of kalata B8 with representative members from Möbius and bracelet subfamilies shows that it is a natural hybrid of the two subfamilies; loops 2 and 3 resemble Möbius sequences, and loop 5 resembles bracelet sequences, as highlighted in *boxes*. The reductive unfolding of kalata B8 (*left*) depicts the unfolding of the native to the reduced form without a characteristic intermediate (*i.e.*, an "all or none" unfolding mechanism). Under standard oxidation condition 9, reduced kalata B8 readily folds to the native conformation (*right*).

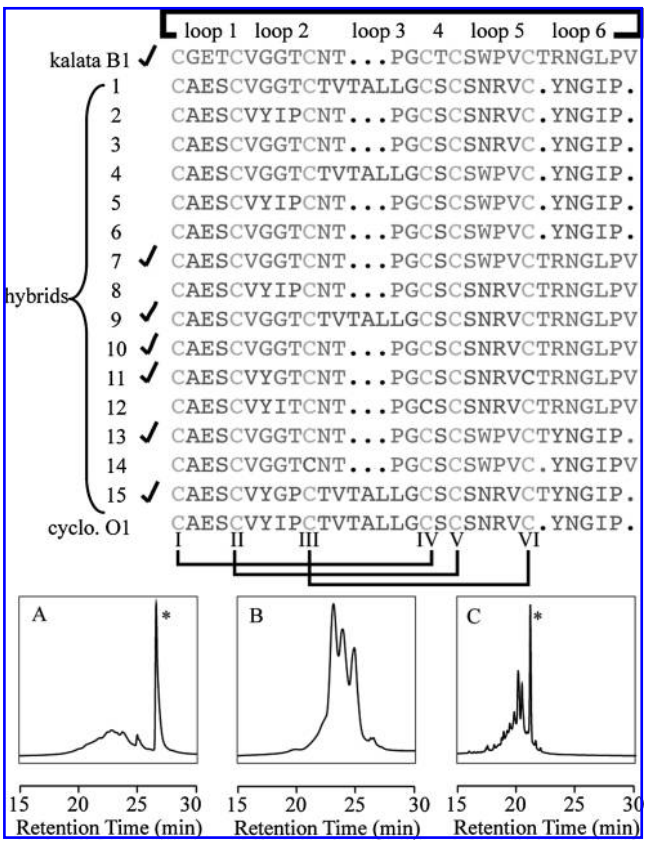

FIG. 3. Sequence alignment of designed Möbius-bracelet hybrids and selected RP-HPLC profiles of hybrids. The sequences of the synthetic hybrid peptides are shown along with inset panels showing HPLC traces of typical folding reactions. The designed hybrids contain a combination of different loops from the two prototypical scaffolds. The sequences highlighted with *ticks* indicate correctly folded analogues. (**A**) Hybrid 13 is a well-folded peptide (indicated by *) formed in high yields. (**B**) Hybrid 6 shows the characteristic pattern for a misfolded peptide consisting of several closely eluting several broader peaks. (**C**) Hybrid 11 is a well-folded peptide (indicated by *), eluting late after a mixture of misfolded isomers.

sequence. As indicated in Fig. 3, this peptide misfolded *in vitro,* indicating that engineering a Möbius loop 2 into a bracelet cyclotide is not sufficient to facilitate folding. Hybrid 2 is a cycloviolacin O1 sequence with loop 3 replaced by the kalata B1 loop 3 sequence. Loop 3 of the bracelet cyclotides is strikingly different in size and sequence from that in Möbius cyclotides. Unlike in the members of the Möbius subfamily, loop 3 is helical in the bracelet subfamily and contains residues that form part of the hydrophobic surface of cyclotides (40). Thus, this region stands out as the most likely region to differentiate the folding pathways of the two subfamilies. Surprisingly, hybrid 2 also misfolded, indicating that the Möbius loop 3 is not sufficient to induce correct folding.

The results from the initial hybrid peptides led us to consider the possibility that the residues that influence folding are embedded in several loops across the sequence and not just confined to a single loop. Thus, we designed hybrid 3, which contains both loops 2 and 3 of cycloviolacin O1, replaced with the corresponding kalata B1 sequences. However, misfolding of this peptide demonstrated that this loop combination does not facilitate correct folding of cycloviolacin O1. Accordingly, we designed several peptides containing other loop combinations. Hybrid 4, containing kalata B1 loops 2 and 5, as well as hybrid 5, which contains kalata B1 loops 3 and 5, both misfolded. Hybrid 6, which contains loops 2, 3, and 5 of kalata B1, also misfolded, indicating that these three loops alone are not sufficient to facilitate folding. However, when loop 6 was also changed into a Möbius sequence (Hybrid 7), the peptide correctly folded (oxidation condition 8), indicating that loop 6 has a major impact on folding. A sharp late-eluting peak characteristic of a well-folded peptide was observed on RP-HPLC, as shown in Fig. 3, and was confirmed to contain correctly folded peptide by ^{1}H-NMR. Specifically, αH chemical shifts are extremely sensitive to structural changes and indicated similarity of this hybrid to native kalata B1 (Fig. 4).

We chose not to modify loops 1 and 4 for any hybrids, as these loops form part of the cystine knot and are tightly conserved across the two cyclotide subfamilies. Thus, they

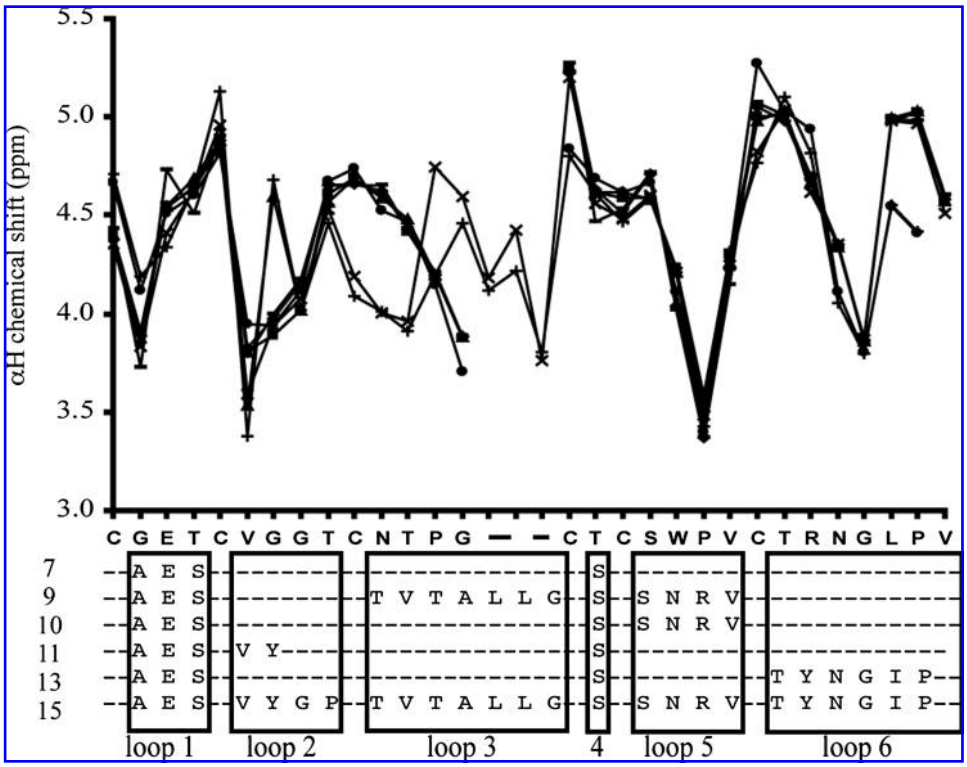

FIG. 4. A comparison of αH chemical shifts of folded hybrid analogues and kalata B1. The αH NMR chemical shifts were derived from analysis of TOCSY and NOESY spectra recorded at 600 MHz, 290 K. The sequence differences for the hybrid from kalata B1 are highlighted below the kalata B1 sequence. Hybrid 11 (*triangle*), hybrid 15 (*vertical line*), hybrid 8 (*cross*), hybrid 10 (*square*), hybrid 7 (*diamond*), kalata B1 (*horizontal line*), hybrid 13 (*circle*). The gaps in the chemical-shift profile result from kalata B1 having fewer residues in loop 3 than does cycloviolacin O1.

were not expected to induce differential folding behavior. This assumption is supported by the fact that hybrid 7 contains bracelet loops 1 and 4, but still folds correctly, unlike most bracelet cyclotides.

Hybrid 8, which contains kalata B1 loops 3 and 6, misfolded, but hybrid 9, which contains kalata B1 loops 2 and 6, gave a prominent late-eluting peak on RP-HPLC (oxidation condition 6) that was confirmed by NMR to contain the correctly folded material. As shown in Fig. 4, the αH chemical shifts of hybrid 9 closely follow those of native kalata B1, indicating that it maintains a native cyclotide conformation.

Overall, it became clear that the presence of certain residues in Möbius loops 2 and 6 synergistically induces correct folding. Further, as hybrid 9 contains bracelet loops 3 and 5, these loops apparently do not cause cyclotides to misfold. These findings for hybrid 9 are quite significant, as they eliminate some of the key misconceptions on bracelet folding (*i.e.*, the misfolding in bracelet cyclotides may be caused by either the helical bracelet loop 3 or the lack of a *cis*-Pro in the bracelet loop 5). The ability to translocate a bracelet loop 3 onto a Möbius scaffold without causing it to misfold suggests that loop 3 is a highly permissive region for modification or bioactive epitope insertion. Supporting inferences were made from hybrid 10, designed by replacing loops 2, 3, and 6 of cycloviolacin O1 with the corresponding kalata B1 sequences. This peptide folded into a native-like conformation (oxidation condition 8), indicating that the presence of bracelet loop 5 does not lead to misfolding. This is consistent with a previous study on kalata B1 analogues that had cationic residues from a bracelet counterpart substituted into loop 5 and correctly folded cyclotide analogues were obtained (9).

The next step was to investigate whether specific residues in loops 2 and 6 influence folding. Loop 2 of kalata B1 contains the sequence VGGT, whereas the corresponding loop in cycloviolacin O1 is VYIP. Hybrid 11, designed to contain the VYGT sequence in loop 2, folded into a native conformation (oxidation condition 1), confirming that the Tyr residue that resides in loop 2 of cycloviolacin O1 is not responsible for misfolding. However, the NMR peaks for the Tyr residue were broadened at 290 K, as were the amide protons of Cys^5, Val^6, Try^7, and Asn^{11}. Additional spectra acquired at higher temperatures (310 K) allowed the observation of all spin systems, but the broadening behavior indicated that the loop 2 with the VYGT sequence is likely to be flexible. Interestingly, when the sequence in loop 2 was altered to VYIT (hybrid 12), the peptide misfolded, indicating that the Ile residue at the third position of this loop is not compatible with folding into the native conformation.

Next we aimed to identify the specific residues in loop 6 that cause misfolding. Comparison of loop 6 sequences across kalata B1 and cycloviolacin O1 revealed that the sequences are quite similar except for the Thr at the start and Val at the end that are missing in cycloviolacin O1. Thus, we wanted to determine whether these missing residues have an impact on folding in the bracelet framework. Hybrid 13 was designed by modifying the hybrid 6 sequence with an extra Thr at the start of loop 6. This small change resulted in a folded peptide (oxidation condition 8), indicating that introducing a Thr residue can facilitate folding. Hybrid 14 designed by introducing a Val at the end of loop 6 of hybrid 6, however, did not fold correctly, indicating that the Val may not have an influence on folding.

To confirm our findings, we made hybrid 15, which is basically the cycloviolacin O1 sequence with the replacement of the Ile with Gly in loop 2 and the addition of a Thr at the start of loop 6. Hybrid 15 readily folded into a native

conformation by using oxidation condition 6, as shown in Fig. 5, and the presence of the cystine knot topology was confirmed from αH chemical shifts (Fig. 4). Thus, overall the data show that loops 2 and 6 in native cycloviolacin O1 are the primary cause of misfolding in bracelet cyclotides, and by two changes to the sequence, an amino acid substitution and an amino acid addition, the natively folded conformation can be rescued.

We also examined the reductive unfolding and oxidative folding pathways of hybrid 15. In the reductive unfolding of hybrid 15, no folding intermediates were seen, as shown in Fig. 5. The peptide was reduced within 10 min in the reduction buffer and resulted in a broad peak on RP-HPLC. The reduced peak for hybrid 15 is significantly broader than that observed for the reduced form of kalata B8, and such broadening on RP-HPLC can indicate the presence of multiple conformations.

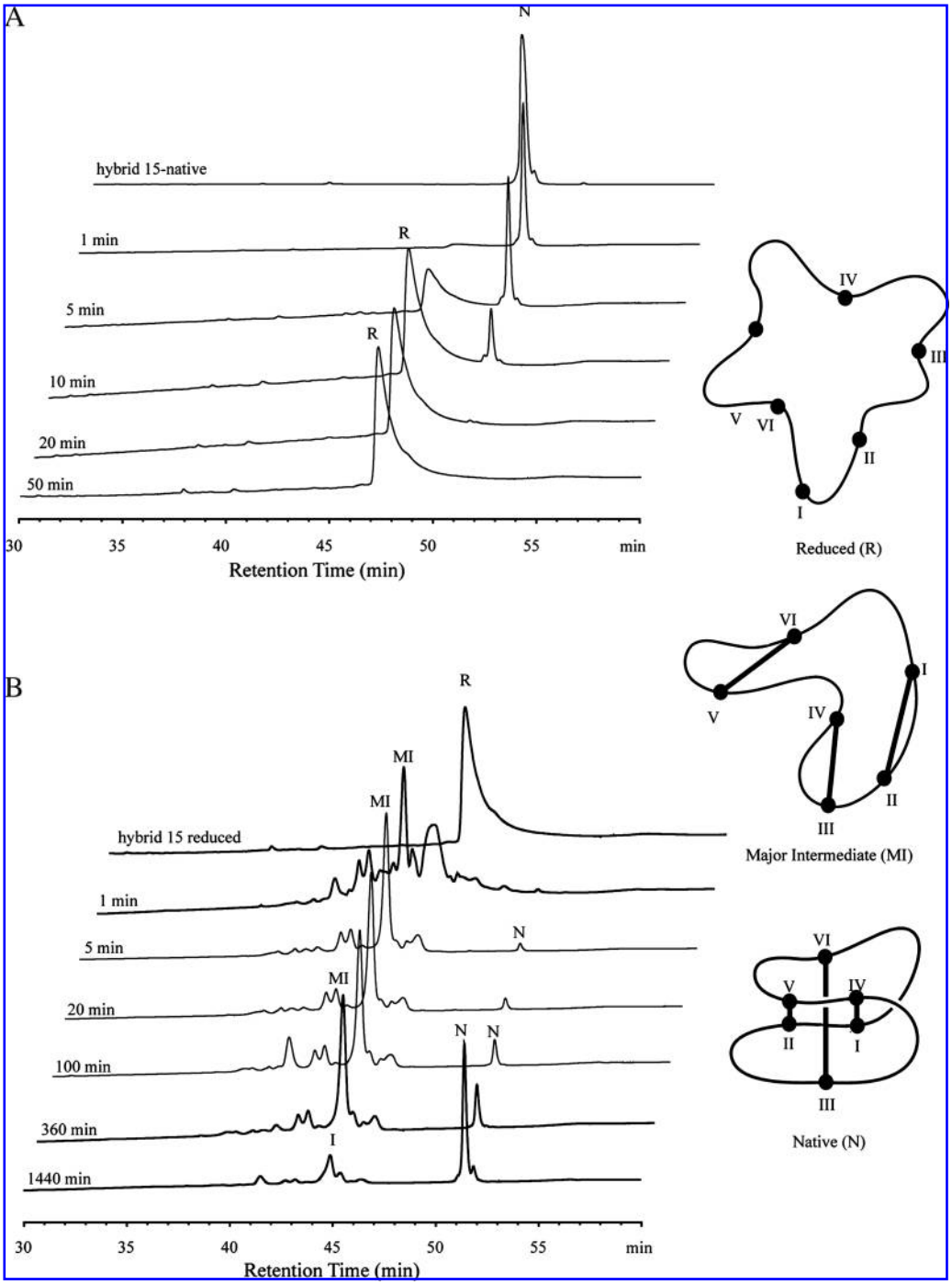

FIG. 5. Oxidative folding and reductive unfolding of hybrid 15. (**A**) In the reductive unfolding of hybrid 15, no folding intermediates are present. (**B**) In the oxidative folding of hybrid 15, a major intermediate (MI) containing three nonnative disulfide bonds is present. MI converts to the native (N) conformation in standard oxidation condition 6. The HPLC traces are offset in the diagram for clarity.

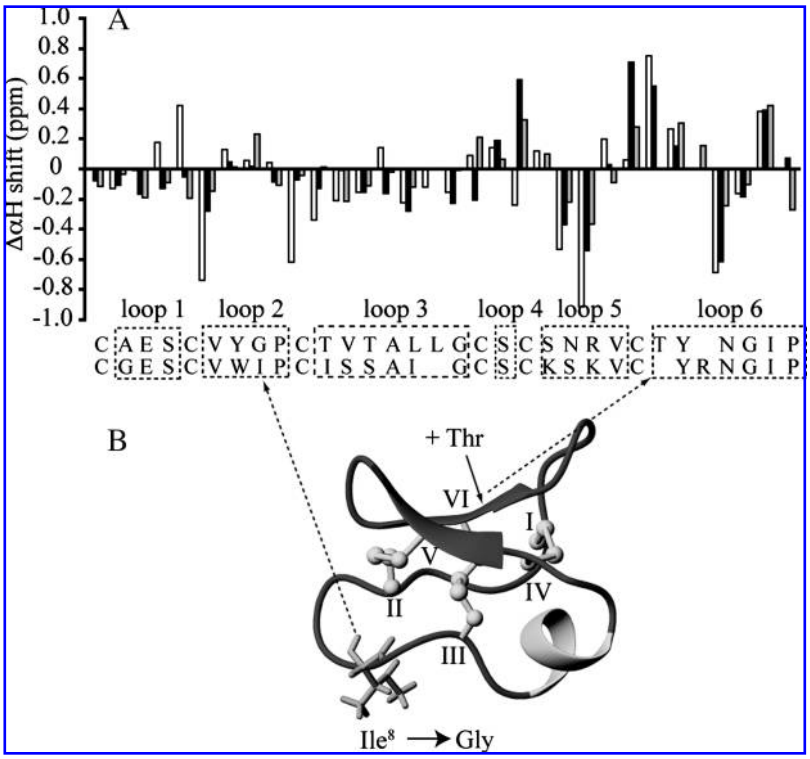

FIG. 6. Comparison of the secondary αH chemical shifts of the major intermediate (MI), native hybrid 15, and the folding intermediate in cycloviolacin O2. (**A**) Comparison of native hybrid 15 (*white*), MI (*black*), and the major intermediate in cycloviolacin O2 (*gray*) (1); the peptide sequence alignment contains hybrid 15 (*top*) and cycloviolacin O2 (*bottom*). (**B**) The structural features of hybrid 15. The two changes from cycloviolacin O1 made in hybrid 15 are highlighted on the structure of cycloviolacin O1; an amino acid substitution was made in loop 2 where the Ile is highlighted, and an amino acid addition was made to loop 6 at the site indicated by an *arrow*.

During oxidative folding of hybrid 15, a major intermediate (MI) was present together with other minor intermediates, as shown in Fig. 5. MI accumulated as the major species during the initial 6 h of folding, and mass analysis indicated that it is a three-disulfide isomer of hybrid 15. Over a 24-h time period, MI converted to the native form.

To gain information on the structure and the disulfide connectivity of MI, we compared the NMR secondary αH chemical shifts of MI, native hybrid 15, and the major intermediate present in the folding pathway of cycloviolacin O2 (1). Secondary shifts reflect the difference in shift of a given residue in a peptide of interest from that of the same residue in a random coil peptide, and in general, the larger the secondary shifts, the more structured the peptide. As is apparent from Fig. 6, the secondary shifts for MI residues in loops 1 to 4 are generally smaller than in the native hybrid 15, suggesting a less-well-defined structure in this region. Indeed, the average secondary shift in this region is <0.2 ppm, which makes the region close to random coil. However, the secondary shifts for loop 5 and 6 residues are very similar to those of the native species, indicating a similar conformation in these loops. Loops 5 and 6 of the prototypical bracelet cyclotide cycloviolacin O1 form a β-hairpin, which is a key element of its secondary structure (40). Specifically, the β-hairpin is formed by strand 1 (residues 19 to 21) and strand 2 (residues 24 to 26), which are linked by a type I β-turn involving residues 21 to 24 (40). The similarity in the secondary shifts of MI and the native conformation of hybrid 15 in loops 5 and 6 suggests that the β-hairpin motif is most likely intact in MI. The two most significant differences in shifts between hybrid 15 and MI are for the Cys residues preceding loops 5 and 6. Given the similarity of all of the other shifts and hence the similar hairpin conformation, the most likely explanation for the differences in Cys secondary shifts is that they have a different (*i.e.*, nonnative) disulfide connectivity in the intermediate compared with the native hybrid 15 structure.

A characteristic three-disulfide isomer with nonnative disulfide bonds is present in the folding pathway of the bracelet cyclotide cycloviolacin O2 (1). As shown in Fig. 6, a similar pattern of secondary shifts is seen for MI and that intermediate in all loops. In the cycloviolacin O2 folding intermediate, disulfide bonds are present between Cys^{I} and Cys^{II}, Cys^{III} and Cys^{IV}, and Cys^{V} and Cys^{VI} (1), and the same nonnative connectivity is likely to be present in MI. Thus, overall, our data suggest that the folding intermediate MI identified in the current study, which is formed early in the folding pathway, has a native-like hairpin structure but has nonnative disulfide bonds and is relatively unstructured in the non-hairpin regions. It appears that the β-hairpin structure is a crucial nucleation locus for protein folding in bracelet cyclotides.

Discussion

In this study, we examined the *in vitro* folding of a series of Möbius:bracelet hybrid cyclotides and determined that two specific loops play a significant role in the folding. Although the Möbius subfamily of cyclotides has previously been shown to fold efficiently into the native conformation *in vitro*, the bracelet cyclotides had until recently proven intractable under a range of standard oxidation conditions. The hybrid cyclotides made for this study were assembled by using solid-phase peptide synthesis with a thioester strategy for forming the cyclic backbone. The folding was examined with RP-HPLC and NMR spectroscopy. Characteristic features observed when the cyclotides folded into their native conformations included late-eluting peaks on HPLC and well-dispersed amide signals in NMR spectra. Analysis of the folding yields of the hybrids indicated that the complexity in the *in vitro*

folding of the bracelet cyclotide cycloviolacin O1 is sequence dependent and is hindered mainly by residues in backbone loops 2 and 6. By substituting a single residue in loop 2, and with the addition of an extra residue in loop 6 to resemble the prototypical Möbius cyclotide kalata B1, it was possible to obtain the native fold for several cyclotide hybrids by using simple *in vitro* folding conditions. The findings from this work are significant because understanding the mechanistic details of the *in vitro* folding in cyclotides is potentially invaluable for protein-engineering applications that use cyclotide scaffolds for the stabilization of bioactive sequences.

We determined that replacement of either loop 2 or loop 6 of cycloviolacin O1 with corresponding kalata sequences, one at a time, does not result in a natively folded conformation. Thus, the contribution of these loops individually to the stability of the native fold is not sufficient to induce correct folding. Correct folding in the hybrids is not promoted unless both loops 2 and 6 are replaced simultaneously with Möbius-like sequences, suggesting the possibility of a synergistic interaction between residues in these loops at some point on the folding pathway or in the final product. The specific residues favorable for folding in the hybrid are a Gly in loop 2 and a Thr in loop 6. The structure in Fig. 6 shows that these residues are remotely located from each other (40), thus excluding their synergistic interaction in the final fold.

Given the lack of a possible synergistic interaction in the final fold, the observed folding data were then examined for fit to other folding models that would implicate these residues, the first being that they play a cumulative role in stabilizing the final structure, thus driving folding on a thermodynamic basis; and the second, that they have synergistic interactions early in the folding process when they might be closer to one another before the final fold takes shape. Structural analysis of kalata B1 shows that Gly^8 in loop 2 has a positive φ angle and is involved in a type I β-turn (40). In native cycloviolacin O1, the Ile^8 that occupies this position has a negative φ angle, even though it is also involved in a type I β-turn. The differences in φ angles suggest that differences exist in the orientation of these residues and hence different local interactions established among neighboring residues. Thus, it is possible that the Gly^8 in the "foldable" hybrids induces a thermodynamically favorable turn in loop 2. In addition, introducing a hydroxyl-bearing Thr may facilitate the formation of hydrogen bonds across the β-hairpin, similar to those observed in kalata B1 (40), which may promote correct folding. Further amino acid replacements, such as substitution of the Thr in loop 6 with a non–hydroxyl containing residue, may provide additional information regarding the role of this residue in folding. However, it appears that the combination of the Gly in loop 2 and the Thr in loop 6 stabilizing factors is the minimal requirement to rescue the otherwise unfavorable *in vitro* folding of bracelet cyclotides.

To examine the possibility that these residues alternatively play a role earlier in the folding pathway, perhaps through mutual synergistic interactions, it was necessary to probe the structure of the nonnative three-disulfide intermediate that accumulates in the folding of hybrid 15. An intermediate with a similar secondary structure was recently reported in the folding of cycloviolacin O2 (1). Interestingly the cycloviolacin O2 intermediate does not readily convert to the native form under standard oxidation conditions and requires very specific folding conditions to convert to the native form. By contrast, the intermediate present in hybrid 15 readily converts to the native form under standard oxidation conditions. It appears that introducing the Gly and Thr changes in loop 2 and 6 modulates the stability of the folding intermediate, enabling it to undergo the disulfide shuffling necessary to convert to the native form.

A chemical-shift analysis of MI and comparison with the cycloviolacin O2 intermediate indicates that the β-hairpin is present in MI and is most likely stabilized by a Cys^{V}-Cys^{VI} disulfide bond. Based on the time course of the folding of hybrid 15, MI appears early in the folding, and thus, the β-hairpin most likely serves as a nucleation site for folding. Furthermore, the early appearance of the hairpin motif, while the rest of the intermediate is relatively unstructured, suggests that the potential hydrogen-bonding interactions of the Thr residue also assist in stabilizing the formation of the hairpin. Because formation of the hairpin effectively precludes a close synergistic interaction of the key Thr and Gly residues, each probably contributes separately but cumulatively to stabilization of the intermediate Thr by stabilizing the nucleating β-hairpin and Gly by assisting in formation of the turn in loop 2 that forms later.

Overall, the folding mechanism developed here first involves formation of a β-hairpin involving loops 5 and 6 that forms early to produce a readily detectable and long-lived intermediate. The intermediate has nonnative disulfide bonds, most likely formed between successive pairs of Cys residues. This suggestion is consistent with an initial kinetically driven formation of disulfide bonds between Cys residues that are closest together in the sequence. The resultant intermediate converts to the native form *via* the formation of a turn in loop 2 and disulfide reshuffling.

It is interesting to note that the residues that were determined to be important for *in vitro* folding are present in the sequence of the "natural chimera," kalata B8 (16). Specifically, a Gly residue at the third position in loop 2 and a Thr at the start of loop 6 are present. The fact that kalata B8 folds into a native conformation *in vitro* further confirms that these residues in loops 2 and 6 have a prominent role in folding.

As the primary amino acid sequence in a protein is thought to dictate its folding mechanism and final topology (3, 19), the question arises as to whether the sequence hypervariability observed in the cyclotides is associated with a large number of folding mechanisms. Alternatively, does the partial sequence conservation observed within each cyclotide subfamily mean that the conserved residues dictate a common mechanism for the subfamily? Detailed oxidative folding pathways have now been determined for a representative member from each of the three cyclotide subfamilies (1, 6, 15). Möbius and trypsin-inhibitor cyclotides have different folding pathways, despite having a common two-disulfide intermediate containing native-like disulfide bonds (6, 15). In Möbius cyclotides, this intermediate, despite having two native disulfide bonds, is not the direct precursor of the native form and requires disulfide reshuffling to convert into the native form (15). The inability to isolate the direct precursor of the native form in the refolding of kalata B1 indicates that it is likely to be a transient intermediate. The intermediate seen for the prototypical trypsin inhibitor cyclotide MCoTI-II directly converts to the native form and appears to be an on-pathway intermediate. As already noted, a recent study that examined the folding bracelet cyclotide, cycloviolacin O2, identified a

three-disulfide intermediate with nonnative bonds as the major species present during folding (1). Other one-disulfide and three-disulfide intermediates were also present as minor products during folding, but no two-disulfide intermediates were seen. Cycloviolacin O2 was also shown not to fold correctly under conditions generally used for kalata B1. Under the folding conditions used in this study, we also observed a suite of misfolded isomers for cycloviolacin O1. Collectively, these results suggest that folding of bracelet cyclotides occurs *via* a pathway that is different from both Möbius and trypsin inhibitor subfamilies, at least *in vitro*.

The folding situation *in vivo* is likely to be more complex still, likely involving folding auxiliaries. For example, a protein disulfide isomerase was recently isolated from the cyclotide-producing plant *Oldenlandia affinis* and shown to facilitate cyclotide folding (26). As well as delineating which residues are important for facilitating folding, the findings from the current study also identified regions within the cyclotide scaffold that are not important for folding and are thus permissive to mutations. This knowledge will facilitate the use of a range of cyclotides, including bracelet cyclotides, as grafting scaffolds in protein-engineering applications.

In summary, the current study has enhanced the information known regarding the folding of cyclotides and has provided a mechanistic insight into cyclotide folding, identifying the specific structural elements that influence correct folding, and demonstrated that they are localized within two intercysteine loops. More generally, the study complements other recent studies on the folding of a wide range of disulfide-rich peptides and proteins (2).

Acknowledgments

This work was supported by a grant from the Australian Research Council (ARC). D.J.C. is an ARC Professorial Fellow. S.G. is grateful for an International Postgraduate Research Scholarship. N.L.D. was supported by a NHMRC industry fellowship. R.J.C. is a NHMRC Biomedical CDA Fellow.

Abbreviations

Boc, *t*-butoxycarbonyl; CCK, cyclic cystine knot; cyclo. O1, cycloviolacin O1; ESI-MS, electrospray ionization mass spectrometry; HF, hydrogen fluoride; HIV, human immunodeficiency virus; MCoTI-I, *Momordica cochinchinenesis* trypsin inhibitor I; MCoTI-II, *Momordica cochinchinenesis* trypsin inhibitor II; NMR, nuclear magnetic resonance spectroscopy; NOESY, nuclear Overhauser enhancement spectroscopy; PAM, phenylacetamidomethyl; RP-HPLC, reverse-phase high-performance liquid chromatography; SFTI-1, sunflower trypsin inhibitor 1; TFA, trifluoroacetic acid; TOCSY, total correlation spectroscopy; Tris-HCl, 2-amino-2(hydroxymethyl)-1,3-propanediol hydrochloride; WATERGATE, water suppression by gradient-tailored excitation.

Author Disclosure Statement

No competing financial interests exist.

References

1. Aboye TL, Clark RJ, Craik DJ, and Goransson U. Ultra-stable peptide scaffolds for protein engineering: synthesis and folding of the circular cystine knotted cyclotide cycloviolacin O2. *ChemBioChem* 9: 103–113, 2008.
2. Arolas JL, Aviles FX, Chang JY, and Ventura S. Folding of small disulfide-rich proteins: clarifying the puzzle. *Trends Biochem Sci* 31: 292–301, 2006.
3. Baker D. A surprising simplicity to protein folding. *Nature* 405: 39–42, 2000.
4. Barbeta BL, Marshall AT, Gillon AD, Craik DJ, and Anderson MA. Plant cyclotides disrupt epithelial cells in the midgut of lepidopteran larvae. *Proc Natl Acad Sci U S A* 105: 1221–1225, 2008.
5. Barry DG, Daly NL, Bokesch HR, Gustafson KR, and Craik DJ. Solution structure of the cyclotide palicourein: implications for the development of a pharmaceutical framework. *Structure* 12: 85–94, 2004.
6. Cemazar M, Daly NL, Haggblad S, Lo KP, Yulyaningsih E, and Craik DJ. Knots in rings: the circular knotted protein *Momordica cochinchinensis* trypsin inhibitor-II folds via a stable two-disulfide intermediate. *J Biol Chem* 281: 8224–8232, 2006.
7. Chiche L, Heitz A, Gelly JC, Gracy J, Chau PTT, Ha PT, Hernandez JF, and Le-Nguyen D. Squash inhibitors: From structural motifs to macrocyclic knottins. *Curr Prot Pept Sci* 5: 341–349, 2004.
8. Christmann A, Walter K, Wentzel A, Krätzner R, and Kolmar H. The cystine knot of a squash-type protease inhibitor as a structural scaffold for *Escherichia coli* cell surface display of conformationally constrained peptides. *Protein Eng* 12: 797–806, 1999.
9. Clark RJ, Daly NL, and Craik DJ. Structural plasticity of the cyclic-cystine-knot framework: implications for biological activity and drug design. *Biochem J* 394: 85–93, 2006.
10. Colgrave ML, Kotze AC, Huang YH, O'Grady J, Simonsen SM, and Craik DJ. Cyclotides: natural, circular plant peptides that possess significant activity against gastrointestinal nematode parasites of sheep. *Biochemistry* 47: 5581–5589, 2008.
11. Craik DJ, Clark RJ, and Daly NL. Potential therapeutic applications of the cyclotides and related cystine knot miniproteins. *Expert Opin Invest Drugs* 16: 595–604, 2007.
12. Craik DJ, Daly NL, Bond T, and Waine C. Plant cyclotides: a unique family of cyclic and knotted proteins that defines the cyclic cystine knot structural motif. *J Mol Biol* 294: 1327–1336, 1999.
13. Craik DJ, Daly NL, Mulvenna J, Plan MR, and Trabi M. Discovery, structure and biological activities of the cyclotides. *Curr Prot Pept Sci* 5: 297–315, 2004.
14. Craik DJ, Simonsen S, and Daly NL. The cyclotides: novel macrocyclic peptides as scaffolds in drug design. *Curr Opin Drug Discov Dev* 5: 251–260, 2002.
15. Daly NL, Clark RJ, and Craik DJ. Disulfide folding pathways of cystine knot proteins: tying the knot within the circular backbone of the cyclotides. *J Biol Chem* 278: 6314–6322, 2003.
16. Daly NL, Clark RJ, Plan MR, and Craik DJ. Kalata B8, a novel antiviral circular protein, exhibits conformational flexibility in the cystine knot motif. *Biochem J* 393: 619–626, 2006.
17. Daly NL, Love S, Alewood PF, and Craik DJ. Chemical synthesis and folding pathways of large cyclic polypeptide: studies of the cystine knot polypeptide kalata B1. *Biochemistry* 38: 10606–10614, 1999.
18. Dawson PE, Muir TW, Clarklewis I, and Kent SBH. Synthesis of proteins by native chemical ligation. *Science* 266: 776–779, 1994.

19. Dobson CM. Protein folding and misfolding. *Nature* 426: 884–890, 2003.
20. Felizmenio-Quimio ME, Daly NL, and Craik DJ. Circular proteins in plants: solution structure of a novel macrocyclic trypsin inhibitor from *Momordica cochinchinensis*. *J Biol Chem* 276: 22875–22882, 2001.
21. Goransson U, Sjogren M, Svangard E, Claeson P, and Bohlin L. Reversible antifouling effect of the cyclotide cycloviolacin O2 against barnacles. *J Nat Prod* 67: 1287–1290, 2004.
22. Gran L. An oxytocic principle found in *Oldenlandia affinis* DC: an indigenous, congolese drug "Kalata-Kalata" used to accelerate delivery. *Medd Nor Farm Selsk* 32: 173–180, 1970.
23. Gran L. Isolation of oxytocic peptides from *Oldenlandia affinis* by solvent extraction of tetraphenylborate complexes and chromatography on Sephadex LH-20. *Lloydia* 36: 207–208, 1973.
24. Gran L, Sandberg F, and Sletten K. *Oldenlandia affinis* (R&S) DC: a plant containing uteroactive peptides used in African traditional medicine. *J Ethnopharmacol* 70: 197–203, 2000.
25. Gruber CW, Cemazar M, Anderson MA, and Craik DJ. Insecticidal plant cyclotides and related cystine knot toxins. *Toxicon* 49: 561–575, 2007.
26. Gruber CW, Cemazar M, Heras B, Martin JL, and Craik DJ. Protein disulfide isomerase: the structure of oxidative folding. *Trends Biochem Sci* 31: 455–464, 2006.
27. Gustafson KR, McKee TC, and Bokesch HR. Anti-HIV cyclotides. *Curr Prot Pept Sci* 5: 331–340, 2004.
28. Gustafson KR, Sowder RC, Henderson LE, Parsons IC, Kashman Y, Cardellina JH, Mcmahon JB, Buckheit RW, Pannell LK, and Boyd MR. Circulin-a and Circulin-B novel HIV: inhibitory macrocyclic peptides from the tropical tree *Chassalia parvifolia*. *J Am Chem Soc* 116: 9337–9338, 1994.
29. Hernandez JF, Gagnon J, Chiche L, Nguyen TM, Andrieu JP, Heitz A, Hong TT, Pham TTC, and Nguyen DL. Squash trypsin inhibitors from *Momordica cochinchinensis* exhibit an atypical macrocyclic structure. *Biochemistry* 39: 5722–5730, 2000.
30. Ireland DC, Colgrave ML, and Craik DJ. A novel suite of cyclotides from *V. odorata*: sequence variation and the implications for structure, function and stability. *J Pept Sci* 12: 143–143, 2006.
31. Jennings C, West J, Waine C, Craik D, and Anderson M. Biosynthesis and insecticidal properties of plant cyclotides: the cyclic knotted proteins from *Oldenlandia affinis*. *Proc Natl Acad Sci U S A* 98: 10614–10619, 2001.
32. Jennings CV, Rosengren KJ, Daly NL, Plan M, Stevens J, Scanlon MJ, Waine C, Norman DG, Anderson MA, and Craik DJ. Isolation, solution structure, and insecticidal activity of Kalata B2, a circular protein with a twist: do Mobius strips exist in nature? *Biochemistry* 44: 851–860, 2005.
33. Koltay A, Daly NL, Gustafson KR, and Craik DJ. Structure of circulin B and implications for antimicrobial activity of the cyclotides. *Int J Pept Res Ther* 11: 99–106, 2005.
34. Leta Aboye T, Clark RJ, Craik DJ, and Goransson U. Ultrastable peptide scaffolds for protein engineering-synthesis and folding of the circular cystine knotted cyclotide cycloviolacin O2. *ChemBioChem* 9: 103–113, 2008.
35. Lindholm P, Goransson U, Johansson S, Claeson P, Gullbo J, Larsson R, Bohlin L, and Backlund A. Cyclotides: a novel type of cytotoxic agents. *Mol Cancer Ther* 1: 365–369, 2002.
36. Mulvenna JP, Wang C, and Craik DJ. CyBase: a database of cyclic protein sequence and structure. *Nucleic Acids Res* 34: D192–D194, 2006.
37. Mulvenna JR, Sando L, and Craik DJ. Processing of a 22 kDa precursor protein to produce the circular protein tricyclon A. *Structure* 13: 691–701, 2005.
38. Plan MR, Saska I, Cagauan AG, and Craik DJ. Backbone cyclised peptides from plants show molluscicidal activity against the rice pest *Pomacea canaliculata* (Golden Apple Snail). *J Agric Food Chem* 56: 5237–5241, 2008.
39. Roberts BL, Markland W, Ley AC, Kent RB, White DW, Guterman SK, and Ladner RC. Directed evolution of a protein: selection of potent neutrophil elastase inhibitors displayed on M13 fusion phage. *Proc Natl Acad Sci U S A* 89: 2429–2433, 1992.
40. Rosengren KJ, Daly NL, Plan MR, Waine C, and Craik DJ. Twists, knots, and rings in proteins: structural definition of the cyclotide framework. *J Biol Chem* 278: 8606–8616, 2003.
41. Schnolzer M, Alewood P, Jones A, Alewood D, and Kent SBH. In situ neutralization in biochemistry solid-phase peptide-synthesis: rapid, high-yield assembly of difficult sequences. *Int J Pept Protein Res* 40: 180–193, 1992.
42. Schöpke T, Hasan Agha MI, Kraft R, Otto A, and Hiller K. Hämolytisch aktive komponenten aus *Viola tricolor* L. und *Viola arvensis* Murray. *Sci Pharm* 61: 145–153, 1993.
43. Simonsen SM, Sando L, Ireland DC, Colgrave ML, Bharathi R, Goransson U, and Craik DJ. A continent of plant defense peptide diversity: cyclotides in Australian *Hybanthus* (Violaceae). *Plant Cell* 17: 3176–3189, 2005.
44. Svangard E, Goransson U, Hocaoglu Z, Gullbo J, Larsson R, Claeson P, and Bohlin L. Cytotoxic cyclotides from *Viola tricolor*. *J Nat Prod* 67: 144–147, 2004.
45. Tam JP and Lu YA. A biomimetic strategy in the synthesis and fragmentation of cyclic protein. *Protein Sci* 7: 1583–1592, 1998.
46. Tam JP, Lu YA, Yang JL, and Chiu KW. An unusual structural motif of antimicrobial peptides containing end-to-end macrocycle and cystine-knot disulfides. *Proc Natl Acad Sci U S A* 96: 8913–8918, 1999.
47. Wang CKL, Kaas Q, Chiche L, and Craik DJ. CyBase: a database of cyclic protein sequences and structures, with applications in protein discovery and engineering. *Nucleic Acids Res* 36: D206–D210, 2008.

Address reprint requests to:
David J. Craik
The University of Queensland
Institute for Molecular Bioscience
Brisbane
QLD 4072, Australia

E-mail: d.craik@imb.uq.edu.au

Date of first submission to ARS Central, September 14, 2008; date of final revised submission, October 30, 2008; date of acceptance, November 17, 2008.

This article has been cited by:

1. Hossein Hashempour, Johannes Koehbach, Norelle L. Daly, Alireza Ghassempour, Christian W. Gruber. 2012. Characterizing circular peptides in mixtures: sequence fragment assembly of cyclotides from a violet plant by MALDI-TOF/TOF mass spectrometry. *Amino Acids* . [CrossRef]
2. Clarence T. T. Wong, Dewi K. Rowlands, Chi-Hang Wong, Theodore W. C. Lo, Giang K. T. Nguyen, Hoi-Yeung Li, James P. Tam. 2012. Orally Active Peptidic Bradykinin B1 Receptor Antagonists Engineered from a Cyclotide Scaffold for Inflammatory Pain Treatment. *Angewandte Chemie International Edition* **51**:23, 5620-5624. [CrossRef]
3. Clarence T. T. Wong, Dewi K. Rowlands, Chi-Hang Wong, Theodore W. C. Lo, Giang K. T. Nguyen, Hoi-Yeung Li, James P. Tam. 2012. Orally Active Peptidic Bradykinin B1 Receptor Antagonists Engineered from a Cyclotide Scaffold for Inflammatory Pain Treatment. *Angewandte Chemie* n/a-n/a. [CrossRef]
4. Clarence T. T. Wong, Misako Taichi, Hideki Nishio, Yuji Nishiuchi, James P. Tam. 2011. Optimal Oxidative Folding of the Novel Antimicrobial Cyclotide from Hedyotis biflora Requires High Alcohol Concentrations. *Biochemistry* 110725134959001. [CrossRef]
5. David J Craik, Anne C Conibear. 2011. The Chemistry of Cyclotides. *The Journal of Organic Chemistry* **76**:12, 4805-4817. [CrossRef]
6. Norelle L. Daly, K. Johan Rosengren, Sónia Troeira Henriques, David J. Craik. 2011. NMR and protein structure in drug design: application to cyclotides and conotoxins. *European Biophysics Journal* **40**:4, 359-370. [CrossRef]
7. Sungkyu Park, Sunithi Gunasekera, Teshome Leta Aboye, Ulf Göransson. 2010. An Efficient Approach for the Total Synthesis of Cyclotides by Microwave Assisted Fmoc-SPPS. *International Journal of Peptide Research and Therapeutics* **16**:3, 167-176. [CrossRef]
8. Richard J. Clark, David J. Craik. 2010. Invited reviewnative chemical ligation applied to the synthesis and bioengineering of circular peptides and proteins. *Biopolymers* **94**:4, 414-422. [CrossRef]
9. Quentin Kaas, David J. Craik. 2010. Analysis and classification of circular proteins in CyBase. *Biopolymers* **94**:5, 584-591. [CrossRef]
10. David J. Craik. 2009. Circling the enemy: cyclic proteins in plant defence. *Trends in Plant Science* **14**:6, 328-335. [CrossRef]